



Addressing Class Imbalance in Soil Movement Predictions

Praveen Kumar¹, Priyanka Priyanka¹, Kala Venkata Uday², Varun Dutt¹

¹Applied Cognitive Science Lab, Indian Institute of Technology Mandi, Himachal Pradesh, 175075, India

²Geotechnical Engineering Lab, Indian Institute of Technology Mandi, Himachal Pradesh, 175075, India

Correspondance to: Praveen Kumar (dr.praveenkumar.ml@gmail.com)

Abstract

Landslides threaten human life and infrastructure, resulting in fatalities and economic losses. Monitoring stations provide valuable data for predicting soil movement, which is crucial in mitigating this threat. Accurately predicting soil movement from monitoring data is challenging due to its complexity and inherent class imbalance. This study proposes developing machine learning (ML) models with oversampling techniques to address the class imbalance issue and develop a robust soil movement prediction system. The dataset, comprising two years (2019-2021) of monitoring data from a landslide in Uttarakhand, was split into a 70:30 ratio for training and testing. To tackle the class imbalance problem, various oversampling techniques, including Synthetic Minority Oversampling Technique (SMOTE), K-Means SMOTE, Borderline SMOTE, Support Vector Machine SMOTE, and Adaptive SMOTE (ADASYN), were applied to the dataset. Several ML models, namely Random Forest (RF), Extreme Gradient Boosting (XGBoost), Light Gradient Boosting Machine (Light GBM), Adaptive Boosting (AdaBoost), Category Boosting (CatBoost), Long Short-Term Memory (LSTM), Multilayer Perceptron (MLP), and dynamic ensemble models, were trained and compared for soil movement prediction. Among these models, the dynamic ensemble model with K-Means SMOTE performed the best in testing, with an accuracy, precision, and recall rate of 99.68% each and an F1-score of 0.9968. The RF model with K-Means SMOTE stood out as the second-best performer, achieving an impressive accuracy, precision, and recall rate of 99.64% each and an F1-score of 0.9964. These results show that ML models with class imbalance techniques have the potential to significantly improve soil movement predictions in landslide-prone areas.

Keywords: Soil Movement Prediction; Class Imbalance; Oversampling; Machine Learning; Landslide Prone Areas.

1. Introduction

Landslides pose a significant threat to infrastructure, resulting in numerous fatalities and substantial economic losses each year (Parkash, 2011). These destructive events occur globally, particularly in hilly and mountainous regions, driven by gravity and characterized by the movement of large rocks, debris, and soil (Crosta, 1998). Factors such as heavy rainfall, earthquakes, and the impacts of climate change contribute to the occurrence and severity of landslides (Crosta, 1998).

Monitoring, predicting, and warning people about slope movements in landslide-prone areas are crucial for mitigating landslide risks. Advanced technologies like GPS, LIDAR, GIS, and remote sensing have proven effective for assessing and analyzing slope failure hazards (Ray et al., 2020). However, their high cost and the need for specialized expertise limit their accessibility, especially in developing countries where cost-effective IoT technologies are necessary (Pathania et al., 2020).

Machine learning (ML) models have been extensively studied for predicting soil movement in landslide-prone areas (Kumar et al., 2021a; Kumar et al., 2021b). This prediction problem could be divided into classification and regression tasks. The classification task aims to predict the degree of soil movement using various ML models. On the other hand, the regression task involves estimating the acceleration or displacement of soil under observation.

One common challenge in landslide prediction is a class imbalance, where certain classes have significantly more data samples than others. This imbalance can adversely affect the performance of ML models. To address class imbalance issues, techniques such as Synthetic Minority Oversampling Technique (SMOTE), K-Means SMOTE, Support Vector Machine SMOTE (SVM-SMOTE), Borderline SMOTE, and Adaptive Synthetic Minority Oversampling Technique (ADASYN) are employed to balance the dataset (Chawla et al., 2002; Douzas et al., 2018; Tang et al., 2008; Han et al., 2005; He et al., 2008).



2

46 Several researchers have dedicated their efforts to addressing class imbalance problems in ML. Notably,
47 Chawla et al. (2002) introduced the SMOTE, Douzas et al. (2018) devised the K-Means SMOTE, Tang et al.
48 (2008) developed the SVM-SMOTE, Han et al. (2005) proposed the Borderline SMOTE, and He et al. (2008)
49 introduced the Adaptive Synthetic Minority Oversampling Technique (ADASYN). These techniques were
50 developed to generate synthetic data and balance imbalanced datasets.

51 The field of soil movement prediction requires further investigation, particularly considering the complexities
52 associated with a class imbalance in the datasets. Despite extensive research on ML models' predictive abilities
53 for soil movement in landslides, there still needs to be more understanding regarding how class imbalance affects
54 the models' performance and accuracy. This study aims to bridge this knowledge gap by examining different
55 approaches to tackle class imbalance and exploring diverse ML models to improve the prediction of soil
56 movement. Various multivariate classification models, including Random Forest (RF), Adaptive Boosting
57 (AdaBoost), Extreme Gradient Boosting (XGBoost), Light Gradient Boosted Machine (Light GBM), Category
58 Boosting (CatBoost), Long Short-Term Memory (LSTM), Multilayer Perceptron (MLP), and an ensemble of
59 RF, AdaBoost, XGBoost, Light GBM, and CatBoost are developed to predict soil movement when coupled with
60 class imbalance techniques (Kumar et al., 2019; Semwal et al., 2022; Wu et al., 2020; Pathania et al., 2021;
61 Zhang et al., 2022; Sahin, 2022; Kumar et al., 2020).

62 This study delves into the field of soil movement prediction, making significant advancements by developing
63 specialized ML models and techniques tailored to this domain. A notable aspect that has received limited
64 attention in the existing literature is the challenge of class imbalance in landslide datasets. While previous
65 research has primarily focused on ML models for soil movement prediction, this work addresses the issue of
66 imbalanced data head-on. Multiple variants of the SMOTE and other balancing strategies are introduced and
67 implemented to enhance the efficacy and accuracy of the ML models.

68 Additionally, this research explores using cost-effective Internet of Things (IoT) technologies in developing
69 regions to improve the investigation and assessment of landslide hazards. The dataset used in this study spans
70 two years, from June 2019 to June 2021, and was collected by an inexpensive IoT monitoring station in
71 Uttarakhand, India. This real-world dataset captures the distinctive characteristics and patterns of soil
72 movements prevalent in the landslide-prone area. By employing a comprehensive methodology, this work
73 advances soil movement prediction and effectively addresses the challenge of class imbalance. It commences
74 with a thorough overview of the collected data, emphasizing the measured weather and soil-related factors.
75 Various SMOTE variants and other balancing techniques are employed to rectify the class imbalance, resulting
76 in the generation of synthetic samples and ensuring a balanced representation of soil movement classes. The
77 intricate correlations and patterns in the soil movement data are captured using a variety of ML models,
78 including RF, AdaBoost, XGBoost, Light GBM, CatBoost, MLP, LSTM, and a dynamic ensembling of RF,
79 AdaBoost, XGBoost, and CatBoost. Overall, this study's findings show potential for accurately reducing
80 landslide risks, increasing the accuracy of landslide prediction, and encouraging the use of cost-effective IoT
81 technologies in landslide-prone locations.

82 **2. Background**

83 Several techniques have been proposed to address the challenge of learning from imbalanced datasets, where
84 the classification categories are not evenly represented. For example, Chawla et al. (2002) proposed the SMOTE,
85 which involves generating synthetic minority class examples to balance the dataset. SMOTE has been shown to
86 improve model performance compared to only undersampling the majority class. Douzas et al. (2018)
87 introduced K-Means SMOTE, a method that combines SMOTE with k-means clustering to effectively overcome
88 imbalances between and within classes without generating unnecessary noise. Tang et al. (2008) modified SVMs
89 by incorporating different rebalancing heuristics, such as cost-sensitive learning, over-sampling, and
90 undersampling. Among the variations of SVM, the granular SVMs-repetitive undersampling model (GSVM-
91 RU) has been found to be the most effective and efficient. Additionally, Han et al., (2005) developed a
92 Borderline SMOTE method that focuses on oversampling only the minority examples near the class boundary.
93 Experimental results indicate that Borderline SMOTE1 and Borderline SMOTE2 outperform SMOTE and



94 random oversampling methods in terms of true positive rate and F-value. Lastly, He et al. (2008) developed the
95 ADASYN, which addresses class imbalance by generating more synthetic data for minority class examples that
96 are harder to learn. ADASYN reduces bias and adaptively shifts the classification decision boundary toward
97 challenging examples. Simulation analyses have demonstrated the effectiveness of ADASYN across various
98 evaluation metrics. These techniques offer valuable approaches to mitigate the impact of imbalanced data in
99 classification tasks. These class imbalance techniques have limited exploration and application for landslide
100 datasets. Existing studies primarily focus on the general imbalanced dataset scenario but need to consider the
101 unique characteristics and challenges associated with landslide datasets. Therefore, research is required for
102 systematic studies that compare the performance and effectiveness of techniques such as SMOTE, K-Means
103 SMOTE, Borderline SMOTE, and ADASYN in the specific context of soil movement prediction across various
104 evaluation metrics. By bridging this literature gap, we can enhance the accuracy and reliability of models for
105 predicting soil movement in landslide-prone areas and contribute to improved landslide risk mitigation
106 strategies.

107 Several researchers developed the various ML models to predict soil movement and prediction problems in
108 other fields (Kumar et al., 2019; Semwal et al., 2022; Wu et al., 2020; Pathania et al., 2021; Zhang et al., 2022;
109 Sahin, 2022; Kumar et al., 2020). For example, Kumar et al. (2019) developed the ensemble of ML models (RF,
110 Bagging, Stacking, and Voting) for predicting soil movement at the Tangni landslide in Uttarakhand, India.
111 These models were compared with Sequential Minimal Optimization (SMO) and Autoregression (AR). The
112 results indicate that the ensemble models outperformed the SMO and AR models in predicting soil movement.
113 Furthermore, Semwal et al. (2022) developed the SMOreg, Instance-based Learning (IBk), RF, Linear
114 Regression (LR), MLP, as well as ensemble ML models to predict root tensile strength for different vegetation
115 species. The results show that the MLP performed better than the other models, providing more accurate
116 predictions of root tensile strength. Next, Wu et al. (2020) developed the decision tree (DT) with AdaBoost and
117 bagging ensembles for mapping the susceptibility of landslides in Longxian County, Shaanxi Province, China.
118 Researcher developed the technique with ensemble of Alternating Decision Tree (ADTree) with Bagging and
119 AdaBoost to map landslide susceptibility. The results revealed that ensemble of ADTree and AdaBoost model
120 performed better than the individual ADTree model and ensemble of ADTree and Bagging model. Similarly,
121 Pathania et al. (2021) developed a novel ensemble gradient boosting model, called SVM-XGBoost, for soil
122 movements warning at Gharpa landslide, Mandi, India. They compared the performance of SVM-XGBoost with
123 other models such as individual SVMs, DTs, RF, XGBoost, Naïve Bayes (NB), and different variants of
124 XGBoost. The results showed that the SVM-XGBoost model performed better than other models in soil
125 movement prediction. In their research, Kumar et al. (2021b) directed their attention toward predicting soil
126 movement, specifically at the Tangni landslide site in India. To enhance the accuracy of their predictions, they
127 explored various variants of Long Short-Term Memory (LSTM) models. They introduced a novel ensemble
128 approach called BS-LSTM, which combined bidirectional and stacked LSTM models. The findings of their
129 study indicated that the BS-LSTM model outperformed the other LSTM variants in accurately predicting soil
130 movement. Similarly, Zhang et al. (2022) conducted a study to assess the susceptibility of landslides using
131 gradient-boosting ML techniques coupled with class-balancing methods. Their investigation specifically
132 focused on the aftermath of the 2018 Hokkaido earthquake and employed diverse datasets and methodologies
133 to predict the susceptibility of specific areas prone to landslides. Compared to well-established models such as
134 XGBoost and Light GBM, the proposed model showcased superior performance in accurately assessing
135 landslide susceptibility. Furthermore, Sahin (2022) developed multiple ML models, including XGBoost,
136 CatBoost, Gradient Boosting Machine (GBM), and Light GBM, to model the susceptibility of landslides. By
137 leveraging a comprehensive landslide inventory map and relevant conditioning factors stored in a geodatabase,
138 the study employed feature selection techniques and compared the predictive capabilities of ensemble methods
139 with the widely used RF model. The results highlighted that CatBoost exhibited the highest predictive capability,
140 followed by XGBoost, Light GBM, and GBM, while RF demonstrated comparatively lower predictive
141 capability. The study used a geodatabase with a landslide inventory map and conditioning factors. Feature
142 selection techniques were applied, and the performance of XGBoost, CatBoost, GBM, and Light GBM was
143 compared to RF. The results revealed that CatBoost had the highest prediction capability, followed by XGBoost,



4

144 Light GBM, and GBM. The literature gap in the context of soil movement prediction is the limited exploration
145 and evaluation of ML models in combination with synthetic data generated by SMOTE techniques. While
146 various ML models, such as ensemble models (e.g., RF), neural networks models (MLP and LSTM), and
147 gradient boosting ML models (e.g., AdaBoost, XGBoost, Light GBM, CatBoost), have been developed and
148 applied for soil movement prediction, their utilization in conjunction with synthetic data generated by SMOTE
149 techniques has received less attention in the literature. Incorporating SMOTE-generated synthetic data into the
150 training process of these models can address the issue of class imbalance in landslide datasets and improve their
151 performance in predicting soil movement. Therefore, further research is needed to investigate the effectiveness
152 of these ML models when combined with SMOTE techniques in the context of soil movement prediction,
153 thereby filling the existing literature gap.

154 The RF, AdaBoost, XGBoost, Light GBM, CatBoost, MLP, LSTM, and an ensemble of RF, AdaBoost,
155 XGBoost, Light GBM, and CatBoost models were chosen to predict soil movement based on their proven
156 effectiveness in previous research. RF is excellent at capturing complex relationships and has outperformed
157 non-ensemble models in predicting debris flow and landslide susceptibility. AdaBoost has successfully
158 predicted soil movement alerts ahead of time. At the same time, XGBoost and Light GBM have demonstrated
159 their ability to achieve balanced and precise predictions, especially in earthquake-induced landslide
160 susceptibility assessments. Among gradient-boosting models, CatBoost stands out for its superior prediction
161 capability, making it a well-suited option for modelling landslide susceptibility. On the other hand, when it
162 comes to predicting root tensile strength, MLP has demonstrated higher accuracy in its predictions. Additionally,
163 LSTM, a robust recurrent neural network architecture, is particularly effective in capturing temporal
164 dependencies and long-term patterns in sequential data. Collectively, these models offer a diverse set of
165 capabilities that prove valuable in the prediction of soil movement.

166 3. Data Collection and Description

167 The dataset for predicting soil movement was collected from an actual landslide site in Uttarakhand, India.
168 Spanning a duration of two years, from June 2019 to June 2021, this dataset holds valuable insights into the
169 behaviour of soil in response to various environmental factors. To gather this data, a cost-effective landslide
170 monitoring station (LMS) was carefully deployed at landslide. Equipped with a range of sensors, the LMS
171 diligently recorded critical weather and soil-related parameters. Weather-wise, it diligently captured temperature
172 readings in degrees Celsius, humidity levels as a percentage, rainfall measurements in inches per hour (in/hr),
173 atmospheric pressure in millibars (mb), and even sunlight intensity in lux. These meticulous recordings shed
174 light on the prevailing weather conditions experienced at the precise location of the landslide. In order to monitor
175 the soil conditions with utmost precision, the LMS relied on an accelerometer sensor. An advanced sensor was
176 utilized to measure the acceleration of the soil in three directions: A_x , A_y , and A_z (in m/s^2). This provided
177 valuable insights into the soil's movement and stability. Additionally, a gyroscope sensor was employed to
178 capture the angular rotation of the soil along the W_x , W_y , and W_z axes (in degrees per second). This sensor
179 enhanced the understanding of the soil's behaviour by accurately detecting its angular movements. Furthermore,
180 the LMS was equipped with a capacitive soil moisture sensor, enabling it to measure the volumetric moisture
181 content of the soil in percentage. The LMS transmitted all these twelve attributes, including weather parameters,
182 soil g-force, angular rotation, and soil moisture content, to the cloud every ten minutes. The dataset obtained
183 from the LMS consisted of approximately thirty-nine thousand data points, covering a wide range of
184 environmental and soil-related attributes. Table 1 is showcasing the statistics for the recorded soil movement
185 prediction parameters. For each attribute, the table provides the mean value, representing the average
186 measurement, along with the standard deviation (Std. Dev.), indicating the variability of the data. The minimum
187 and maximum values highlight the range of measurements observed, offering insights into the extreme values
188 and overall data distribution.



189 **Table 1.** Summary statistics of recorded parameters for soil movement prediction dataset.

Parameter	Mean	Std. Dev.	Min	Max
Temperature (°C)	16.18	10.48	0.00	39.00
Humidity (%)	66.69	35.46	0.00	99.00
Rain (in/hr)	0.00	5.60	0.00	15.00
Pressure (mb)	1040.96	27.96	921.61	1065.41
Light (lux)	5025.35	10154.75	0.00	54612.00
Ax (m/s ²)	0.02	1.23	-28.02	40.25
Ay (m/s ²)	0.00	1.37	-100.08	100.08
Az (m/s ²)	0.00	2.28	-149.61	315.61
Wx (°/s)	0.00	15.86	-1994.51	1997.24
Wy (°/s)	0.00	15.85	-1998.05	1998.73
Wz (°/s)	0.00	6.95	-932.00	932.00
Moisture (%)	80.00	20.30	40.00	100.00

190

191 4. Methodology

192 4.1. Data Pre-processing

193 The sensors installed at the landslide locations experienced malfunctions, resulting in multiple missing values
 194 within the collected data. To address this issue, we employed a method to fill these gaps by replacing the missing
 195 values with the average values recorded at the corresponding timestamps during the previous week. By
 196 calculating the average values for parameters such as light intensity, humidity, temperature, and pressure from
 197 the same time periods in the preceding week, we obtained estimates to replace the skewed or missing data points.

198 4.2. Class Labeling

199 The dataset contained values for acceleration and angular rotation in three directions: x, y, and z. The changes
 200 in acceleration and angular rotation were calculated by subtracting the current values from the past values,
 201 allowing for the assessment of movement. To classify the movement data, four categories were defined: no
 202 movement, low movement, moderate movement, and high movement. These categories were determined based
 203 on standard deviation thresholds derived from the acceleration and angular rotation values. Specifically, values
 204 within ± 1 standard deviation from the mean were categorized as no movement, ± 2 standard deviations as low
 205 movement, ± 3 standard deviations as moderate movement, and values exceeding ± 3 standard deviations as
 206 high movement. This classification approach considered the variability in acceleration and angular rotation
 207 changes to determine the intensity of movement.

208 During the analysis, each timestamp was assigned to a movement class based on the class associated with
 209 the highest standard deviation observed in any acceleration or angular rotation element. If an individual element
 210 had the highest standard deviation at a specific timestamp, that timestamp was assigned to the corresponding
 211 movement class with the maximum standard deviation.

212 Table 2 presents the distribution of movement intensity within the dataset, which consisted of 38,900 data
 213 points. The table shows the percentage distribution of movement categories: high, moderate, low, and no
 214 movement. The majority of the dataset (97.8%) falls under the "No Movement" category, indicating a lack of
 215 significant movement. On the other hand, the high movement category represents only a small fraction (1.1%)
 216 of the dataset. This distribution highlights the class imbalance issue present in the dataset, which needs to be
 217 taken into account when developing a classification model for predicting soil movement.



6

218 **Table 2.** Class distribution of soil movement data points.

Movement Class	Number of Data Points	Percentage
High Movement	423	1.1%
Moderate Movement	146	0.7%
Low Movement	268	0.4%
No Movement	38063	97.8%

219 **4.3. Sliding Window Packets**

220 The sliding window packets technique involves dividing a given dataset into fixed-length subsequences or
221 packets and their corresponding labels. To achieve this, a sequence length parameter is used to determine the
222 length of each subsequence. The sliding window approach is then employed, where a window starts at the
223 beginning of the dataset and moves through the data with a step size of 1. A subsequence of the specified length
224 is extracted from the dataset at each window position. The label for prediction is taken from the next position
225 after the window.

226 The sliding window packets technique aims to predict future values or events based on preceding
227 subsequences. For instance, if the sequence length is set to five, the sliding window will select five consecutive
228 values from the dataset as a subsequence at each step. The label for prediction will be the value at the sixth
229 position. This process continues until the end of the dataset is reached, resulting in multiple subsequences and
230 their respective labels. Once the packets are created, they are flattened to form a single feature vector. For
231 instance, if the sequence length is five and the dataset has twelve features, each packet will contain sixty
232 elements (5x12). This transformation allows the packets to be treated as individual samples with multiple
233 features suitable for ML models. The primary purpose of creating these packets is to address prediction tasks
234 involving sequences where the input data's order and dependencies are crucial. The model can effectively
235 capture and learn patterns and relationships within the sequential data by utilizing the sliding window packets.
236 The flattened packets generated using the sliding window technique are inputs in oversampling techniques.

237 **4.4. Oversampling**

238 In our analysis, we encountered a significant class imbalance issue in the labelled data. The "No Movement"
239 class, which represents the majority of the data, had a large number of data points. On the other hand, the "High
240 Movement" class, which represents the minority class, had only a minimal representation with just 1% of the
241 total data. This class imbalance posed a challenge for building an effective classification model, as the skewed
242 data distribution made it difficult to classify the minority class accurately.

243 To overcome the class imbalance challenge, we implemented several oversampling techniques, with a
244 particular focus on SMOTE and its extensions (Chawla et al., 2002; Douzas et al., 2018; Tang et al., 2008; Han
245 et al., 2005; He et al., 2008). SMOTE, which stands for Synthetic Minority Oversampling Technique, addresses
246 the imbalance by generating synthetic data points for the minority class (Chawla et al., 2002). By utilizing the
247 characteristics of existing samples from the minority class, we created new data points, thereby increasing the
248 representation of the "High Movement" class. In addition to the standard SMOTE, we also explored other
249 variations such as K-Means SMOTE (Douzas et al., 2018), SVM-SMOTE (Tang et al., 2008), and Borderline
250 SMOTE (Han et al., 2005) to further enhance the balance of class distribution.

251 Furthermore, we utilized the ADASYN, an extension of SMOTE that explicitly addresses the classification
252 boundary of the minority class (He et al., 2008). ADASYN assigns higher weights to the minority examples that
253 are more challenging to classify, leading to the generation of additional artificial data points for these instances.
254 By incorporating ADASYN into our oversampling strategy, we enhanced the balance of the class distribution
255 further and improved the classification accuracy for all classes.



256 Fig. 1. illustrates the application of the K-Mean SMOTE technique for addressing the class imbalance. The
 257 figure depicts a scatter plot where the red crosses represent the minority class samples, while the black dots
 258 represent the majority class samples. The green crosses indicate the newly generated synthetic samples by the
 259 K-Mean SMOTE algorithm. The dashed line represents the decision boundary separating the two classes. K-
 260 Mean SMOTE operates by following two simple steps iteratively [8]. Firstly, it assigns each observation to the
 261 nearest cluster centroid among the k available. Secondly, it updates the position of the centroids so that they are
 262 positioned at the centre between the assigned observations. The information ratio (IR) shown in Fig. 1 helps K-
 263 Means SMOTE determine the appropriate amount of oversampling for the minority class, ensuring a balanced
 264 representation of the classes in synthetic samples. The value of k was selected 4 in this experiment.

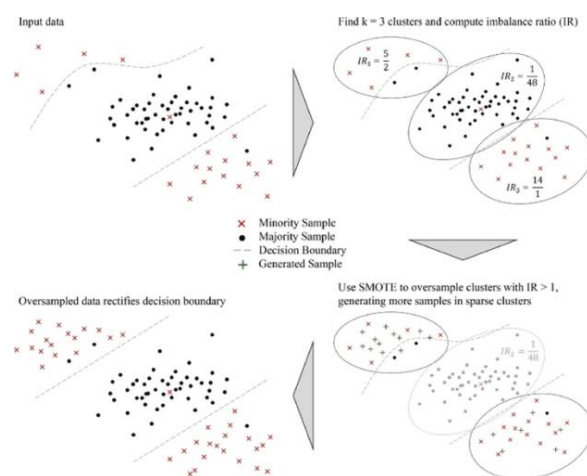


Figure 1. K-Means SMOTE effectively addresses within-class imbalance by oversampling safe areas (Douzas et al., 2018).

265 4.5. Machine Learning Models

266 Various models were employed to classify the soil movement. The specific models will be discussed in the
 267 following subsection. To evaluate the accuracy of these models, the dataset was divided into two groups: training
 268 data (70%) and testing data (30%). Random sampling was used to select 70% of the data points for training the
 269 classification models mentioned below, while the remaining 30% of the dataset was reserved for model
 270 evaluation.

271 4.5.1. AdaBoost

272 AdaBoost, also known as Adaptive Boosting, is a probabilistic classification meta-model designed to enhance
 273 the performance of ML models (Wu et al., 2020). It achieves this by combining the results of multiple weak
 274 learners, which are learning techniques with slightly better than random guessing capabilities. Through an
 275 adaptive process, AdaBoost adjusts subsequent weak models to focus on the cases that were misclassified by
 276 earlier models. This adaptive nature helps improve the overall accuracy of the model and reduces the risk of
 277 overfitting in certain situations. Although individual weak learners may not perform well on their own, their
 278 collective strength allows the final model to converge as a powerful learner capable of making more accurate
 279 predictions.

280 For the AdaBoost model, the number of trees determines the maximum number of weak models to be
 281 combined. Increasing the number of trees can improve the performance of the AdaBoost but may also increase
 282 the risk of overfitting. The learning rate controls the contribution of each weak model, with a higher learning
 283 rate giving more weight to each model. The maximum depth parameter limits the depth of individual weak



284 models, preventing them from becoming too complex and overfitting the data. Table 3 shows the range of
285 hyperparameters for the AdaBoost model.

286 **4.5.2. XGBoost**

287 XGBoost is an ensemble ML model based on gradient boosting and uses decision trees (Chen and Guestrin,
288 2016). While deep neural networks excel in predicting unstructured data such as images and text, decision tree-
289 based methods are considered superior for dealing with structured data. Decision trees are particularly effective
290 when the data has a well-defined structure or specific features, making them a preferred choice for certain
291 prediction problems involving structured information.

292 In the XGBoost model, the number of trees determines the number of boosting rounds or iterations.
293 Increasing the number of trees can improve the performance of XGBoost but also increases computational
294 complexity. The learning rate controls the step size during the boosting process and affects the model's
295 convergence speed and generalization ability. The maximum depth parameter restricts the depth of the decision
296 trees in the ensemble, preventing overfitting and promoting interpretability. Table 3 shows the range of
297 hyperparameters for the XGBoost model.

298 **4.5.3. Light GBM**

299 Light GBM is a gradient-boosting framework that utilizes a decision-branching technique for various ML
300 tasks such as ranking and classification (Ke et al., 2017). Unlike other boosting methods that divide the tree
301 lengthwise or layerwise, Light GBM employs a leaf-wise approach, where the tree is divided leaf by leaf,
302 selecting the best split at each step. The leaf-wise strategy employed in Light GBM offers advantages over
303 traditional boosting techniques by reducing loss and improving accuracy. This strategy focuses on growing the
304 tree leaf-wise rather than level-wise, resulting in a more effective learning process. Light GBM's efficient
305 implementation is reflected in its speedy execution, earning it the moniker "Light" due to its fast performance.

306 In the Light GBM model, the number of trees determines the number of boosting rounds, and increasing this
307 number has the potential to enhance the model's performance. The learning rate parameter influences the step
308 size taken during the boosting process, striking a balance between convergence speed and model accuracy. To
309 control the complexity of the model and mitigate the risk of overfitting, the maximum depth parameter limits
310 the depth of the decision trees employed by Light GBM.

311 Table 3 provides an overview of the hyperparameters range for the Light GBM model, allowing for fine-
312 tuning and customization to optimize its performance according to the specific dataset and problem at hand.

313 **4.5.4. CatBoost**

314 CatBoost, which stands for Category Boosting, is an ML model developed by Yandex and recently released
315 as an open-source tool (Prokhorenkova et al., 2018). Its integration capabilities with popular frameworks like
316 TensorFlow and Core ML make it highly adaptable across different platforms. CatBoost excels in handling
317 diverse datasets, making it a valuable tool for addressing various industry problems. This model's exceptional
318 performance and predictive accuracy contribute to its reputation as a leading choice in the field.

319 The loss function selection is important in the CatBoost model, as it can significantly impact its performance.
320 Different loss functions, such as log, entropy, or hinge, are tailored to handle specific classification problems,
321 and their selection can lead to varying results. To fine-tune the CatBoost model and optimize its performance
322 for a given dataset, Table 3 presents the range of hyperparameters that can be adjusted according to the specific
323 problem and data characteristics.

324 **4.5.5. Random Forest**

325 The RF technique, an ensemble learning method combining predictions from multiple decision trees
326 (Breiman, 2001), was used to construct the regression or classification model. RF offers advantages such as
327 handling relationships and non-linearities without requiring variable independence assumptions or dummy
328 variables. It has shown exceptional performance in various industries and applications, including landslide
329 prediction and site recognition.



330 The RF model's performance is optimized by adjusting parameters such as the number of trees (DTs), the
331 splitting criteria (Gini or Entropy), and the maximum depth of the trees. These parameters control the model's
332 robustness, accuracy, and complexity. Table 3 outlines the hyperparameter ranges for the RF model.

333 **4.5.6. Multilayer Perceptron**

334 The MLP (Multilayer Perceptron) is a well-known neural network architecture (Rosenblatt, 1961). It
335 comprises interconnected layers, including input, hidden, and output layers. Neurons in the MLP calculate a
336 weighted sum of inputs and pass it through an activation function to capture intricate relationships. The hidden
337 layers extract valuable features from the input data. Dropout layers are employed to prevent overfitting by
338 randomly deactivating neurons during training, enhancing the MLP's ability to generalize and reducing reliance
339 on specific patterns. The MLP is a versatile and powerful approach for tackling classification problems.

340 In the MLP model, the look-back period determines the number of preceding time steps considered for
341 prediction, influencing the model's capacity to capture temporal dependencies. The number of layers and nodes
342 per layer govern the complexity of the network and its ability to learn intricate representations from the data.
343 Table 3 provides an overview of the hyperparameter ranges for the MLP model.

344 **4.5.7. LSTM**

345 The LSTM is a recurrent neural network architecture (Hochreiter and Schmidhuber, 1997). It addresses the
346 vanishing gradient problem and analyses sequential data by capturing long-term dependencies. The key strength
347 of LSTM lies in its ability to process and predict sequences of varying lengths. LSTM networks selectively
348 retain or forget information over time by utilizing memory cells and gating mechanisms. As a result, they have
349 proven effective in various domains, including natural language processing, speech recognition, and time series
350 forecasting.

351 In our LSTM model, we conducted experiments to examine the impact of different parameters on its
352 performance. We investigated the influence of various LSTM unit sizes (32, 64, 128, and 256) to understand
353 how the complexity of the model affects its capacity to capture patterns in the data. Additionally, we explored
354 different activation functions (sigmoid, tanh, and ReLU) to assess their effect on the model's ability to learn
355 complex relationships within the dataset. We selected the categorical cross-entropy loss function for multi-class
356 classification tasks due to its suitability. Furthermore, we varied the look-back period from 3 to 10 to evaluate
357 how it influences the model's ability to capture temporal dependencies. The range of hyperparameters for the
358 LSTM model is presented in Table 3.

359 **4.5.8. Dynamic Ensembling**

360 Dynamic ensembling is a highly effective technique in ML that takes advantage of the adaptability and
361 ongoing improvement of predictive models (Ko et al., 2008). It involves creating a versatile and continuously
362 evolving ensemble by harnessing the strengths of multiple models, including RF, CatBoost, XGBoost, Light
363 GBM, and AdaBoost. Traditionally, ensembling methods like bagging and boosting have focused on fixed
364 ensembles. However, dynamic ensembling goes beyond this by introducing the ability to add or remove models
365 based on their performance dynamically. In the case of dynamic ensembling with the models, as mentioned
366 earlier, the monitoring criterion used is accuracy. Accuracy as the monitoring criterion ensures that the dynamic
367 ensemble maintains a high level of accuracy in its predictions. If a model falls below a predefined accuracy
368 threshold, it is considered underperforming and may be replaced to enhance the ensemble's overall performance.

369 Dynamic ensembling offers numerous advantages, including handling concept drift, where the underlying
370 data distribution changes over time. By incorporating new models that capture updated patterns and relationships
371 in the data, the dynamic ensemble can effectively adapt to concept drift and maintain accurate predictions.

372 The dynamic ensembling model utilized base models such as RF, CatBoost, XGBoost, Light GBM, and
373 AdaBoost. Each base model was trained individually with the same default parameter settings as their standalone
374 counterparts. The parameter values for each model were mentioned in Table 3.



375 **Table 3.** The range of hyperparameters varied in the models.

Model	Hyperparameter	Range of Hyperparameter
AdaBoost	Number of Trees	[15, 200] in steps of 10
	Learning Rate	[0.1, 2] in steps of 0.1
	Maximum Depth	[3, 33] in steps of 3
XGBoost	Number of Trees	[50, 1100] in steps of 50
	Learning Rate	[0.05, 0.55] in steps of 0.05
	Maximum Depth	[3, 33] in steps of 3
Light GBM	Number of Trees	[20, 400] in steps of 20
	Learning Rate	[0.05, 0.55] in steps of 0.05
	Max Depth	[3, 33] in steps of 3
CatBoost	Loss Function	Log, Entropy, Hinge
	Learning Rate	[0.1, 2] in steps of 0.1
	Max Depth	[3, 33] in steps of 3
RF	Number of Trees	[1, 100] in steps of 5
	Criteria	Gini, Entropy
	Maximum Depth	[1, 100] in steps of 5
MLP	Look-back Period	3 to 10
	Layers	[1, 3]
	Nodes Per Layer	[50, 250] in steps of 50
LSTM	Look-back Period	3 to 10
	LSTM Units	32, 64, 128, 256
	Activation Function	Sigmoid, tanh, ReLU

376 **5. Model Execution, Minimization, and Handling Class Imbalance**

377 A rigorous process was followed to develop an effective model for predicting the intensity of soil movement.
 378 The model was trained using grid search techniques, which systematically explored different combinations of
 379 hyperparameters to optimize its performance. The training phase utilized the labelled training data, split into a
 380 70:30 ratio for training and testing purposes. One challenge encountered during the training process was the
 381 class imbalance issue. The number of samples available for the minority class was insufficient compared to the
 382 majority class. To address this, oversampling techniques were employed. By generating synthetic data points
 383 for the minority class, we were able to balance the dataset and mitigate the bias toward the majority class. Once
 384 the dataset was balanced, multiple ML models were trained using the training data. The primary objective was
 385 to optimize the models' parameters for improved performance. Each model underwent a grid search to identify
 386 the best configurations, a systematic approach that explores various parameter combinations. The models were
 387 then trained using the optimized parameters and evaluated on independent test data to assess their predictive
 388 performance. The evaluation primarily focused on accuracy metrics to determine how effectively the models
 389 predicted the intensity of soil movement.

390 **6. Results**

391 Table 3 presents the optimized hyperparameter values obtained through the grid search method for each
 392 model. These hyperparameters were carefully fine-tuned to ensure the best fit for the given data. In the case of
 393 XGBoost, the optimized values included 800 trees, a learning rate of 0.3, and a maximum depth of 9. After a



394 thorough evaluation, these parameter settings were selected to improve the model's generalization capability
 395 and ability to capture intricate patterns within the data. The optimized values for the Light GBM model consisted
 396 of 220 trees, a hidden layer size of 0.25, and a maximum depth of 12. These settings were determined to enhance
 397 the model's performance in terms of both speed and accuracy.

398 Similarly, the AdaBoost model underwent hyperparameter optimization, selecting 25 trees, a learning rate of
 399 1.7, and a maximum depth of 20. These parameter values were chosen to improve the model's adaptability and
 400 accuracy for classification tasks. The CatBoost model also went through optimization, leading to entropy
 401 selection as the loss function, a learning rate of 0.9, and a maximum depth of 20. These settings were explicitly
 402 chosen to maximize the model's accuracy and robustness. Likewise, the MLP model optimized its
 403 hyperparameters with a look-back period of 3, 2 layers, and 200 nodes per layer. These settings were selected
 404 to enhance the model's ability to capture complex relationships and improve classification accuracy. Similarly,
 405 LSTM has 128 units and tanh activation function. In the RF model, the optimized values were 45 for the number
 406 of trees, 25 for the maximum depth, and the evaluation criteria were set to "entropy." These values were chosen
 407 to maximize the model's accuracy and predictive power performance. Lastly, the dynamic ensembling model in
 408 this study incorporated the optimized RF, CatBoost, XGBoost, Light GBM, and AdaBoost models to improve
 409 the accuracy of landslide analysis predictions. By leveraging the strengths of these individually optimized
 410 models, as mentioned above, the dynamic ensembling model aimed to improve the accuracy and reliability of
 411 landslide analysis predictions.

412 **Table 4.** The best value of the hyperparameters calibrated from the training data.

Model	Hyperparameter	Best Value of Hyperparameter
AdaBoost	Number of Trees	25
	Learning Rate	1.7
	Maximum Depth	20
XGBoost	Number of Trees	800
	Learning Rate	0.3
	Maximum Depth	9
Light GBM	Number of Trees	220
	Learning Rate	0.25
	Maximum Depth	12
CatBoost	Loss Function	Entropy
	Learning Rate	0.9
	Maximum Depth	20
RF	Number of Trees	45
	Criteria	Entropy
	Maximum Depth	25
MLP	Look-back Period	3
	Layers	2
	Nodes Per Layer	200
LSTM	Look-back Period	5
	LSTM Units	128
	Activation Function	tanh



414 Table 5 presents the training results of different classification models combined with various oversampling
 415 techniques for landslide prediction. These results provide valuable insights into the performance of each model
 416 when trained on the dataset with oversampling. The RF model with K-Mean SMOTE emerges as the best model
 417 in training, achieving outstanding accuracy, precision, recall, and F1-score of 100% and 1, respectively. It
 418 demonstrates remarkable predictive capability by achieving perfect accuracy in both oversampling and non-
 419 oversampling scenarios.

420 Table 6 presents the test results of various classification models combined with different oversampling
 421 techniques for landslide prediction. Among them, the dynamic ensemble model utilizing the K-Mean SMOTE
 422 technique demonstrates exceptional performance in accurately predicting landslides on unseen data. It achieves
 423 impressive accuracy, precision, and recall rates of 99.68%, along with an F1-score of 0.9968. These outstanding
 424 results confirm the effectiveness of the dynamic ensemble approach when combined with K-Mean SMOTE for
 425 accurate landslide prediction. The best-performing model is highlighted in bold in Table 6.

426 Additionally, the RF model incorporating K-Mean SMOTE emerges as the second-best model in the test
 427 phase, showcasing high accuracy, precision, and recall rates of 99.64%, along with an F1-score of 0.9964. This
 428 result emphasizes the reliability and robustness of the RF model in tackling landslide prediction tasks.

429 Comparing the dynamic ensemble and RF models with other classification models and oversampling
 430 techniques, it becomes evident that the dynamic ensemble model with K-Mean SMOTE and the RF model with
 431 K-Mean SMOTE consistently outperform the rest, highlighting their effectiveness in accurately predicting
 432 landslides.

433 These findings underscore the importance of carefully selecting appropriate ML models and employing
 434 suitable oversampling techniques to address the class imbalance challenge in landslide prediction. They provide
 435 valuable insights into the performance and suitability of these models and techniques for enhancing landslide
 436 prediction accuracy, ultimately enabling proactive measures to mitigate landslide risks.

437 **Table 5.** The results of the ML models from training dataset.

Model	Oversampling Technique	Accuracy (in %)	Precision (in %)	Recall (in %)	F1-Score
AdaBoost	SMOTE	71.45	71.41	71.45	0.7142
	K-Means SMOTE	71.13	71.07	71.13	0.7105
	Borderline SMOTE	77.54	77.48	77.54	0.7748
	ADASYN	72.97	72.91	72.97	0.7276
	Without Oversampling	97.87	97.73	97.87	0.9779
CatBoost	SMOTE	99.85	99.85	99.85	0.9985
	K-Means SMOTE	99.86	99.86	99.86	0.9986
	Borderline SMOTE	99.78	99.78	99.78	0.9978
	ADASYN	99.85	99.85	99.85	0.9985
	Without Oversampling	99.72	99.72	99.72	0.9971
XGBoost	SMOTE	99.97	99.97	99.97	0.9997
	K-Means SMOTE	99.98	99.98	99.98	0.9998
	Borderline SMOTE	99.98	99.98	99.98	0.9998
	ADASYN	99.97	99.97	99.97	0.9997
	Without Oversampling	99.99	99.99	99.99	0.9999
Light GBM	SMOTE	99.87	99.87	99.87	0.9987
	K-Means SMOTE	99.91	99.91	99.91	0.9991
	Borderline SMOTE	99.97	99.97	99.97	0.9997
	ADASYN	99.88	99.88	99.88	0.9988
	Without Oversampling	99.87	99.87	99.87	0.9987
RF	SMOTE	100	100	100	1
	K-Means SMOTE	100	100	100	1
	Borderline SMOTE	100	100	100	1



	ADASYN	100	100	100	1
	Without Oversampling	100	100	100	1
MLP	SMOTE	90.32	90.49	90.32	0.9028
	K-Means SMOTE	60.16	73.24	60.16	0.5785
	Borderline SMOTE	95.66	95.72	95.66	0.9566
	ADASYN	88.54	88.81	88.54	0.8854
	Without Oversampling	97.81	96.43	97.81	0.9694
LSTM	SMOTE	68.73	68.81	68.73	0.6799
	K-Means SMOTE	79.51	79.89	79.51	0.7959
	Borderline SMOTE	86.40	86.66	86.40	0.8627
	ADASYN	77.47	77.72	77.47	0.7736
	Without Oversampling	97.88	95.80	97.87	0.9683
Ensemble	SMOTE	99.94	99.94	99.94	0.9994
	K-Means SMOTE	99.96	99.96	99.96	0.9996
	Borderline SMOTE	99.97	99.97	99.97	0.9997
	ADASYN	99.93	99.93	99.93	0.9993
	Without Oversampling	99.99	99.99	99.99	0.9999

438 **Table 6.** The results of the ML models from test dataset.

Model	Oversampling Technique	Accuracy (in %)	Precision (in %)	Recall (in %)	F1-Score
AdaBoost	SMOTE	71.57	71.54	71.57	0.7155
	K-Means SMOTE	71.03	70.89	71.03	0.7091
	Borderline SMOTE	77.65	77.57	77.65	0.7757
	ADASYN	72.83	72.77	72.83	0.7263
	Without Oversampling	97.59	97.41	97.59	0.9749
CatBoost	SMOTE	99.56	99.56	99.56	0.9956
	K-Means SMOTE	99.57	99.57	99.57	0.9957
	Borderline SMOTE	99.50	99.50	99.50	0.9950
	ADASYN	99.58	99.58	99.58	0.9957
	Without Oversampling	98.11	97.85	98.11	0.9787
XGBoost	SMOTE	99.63	99.63	99.63	0.9963
	K-Means SMOTE	99.62	99.62	99.62	0.9962
	Borderline SMOTE	99.57	99.57	99.57	0.9957
	ADASYN	99.64	99.64	99.64	0.9964
	Without Oversampling	98.09	97.63	98.09	0.9775
Light GBM	SMOTE	99.55	99.55	99.55	0.9955
	K-Means SMOTE	99.60	99.60	99.60	0.9960
	Borderline SMOTE	99.54	99.54	99.54	0.9954
	ADASYN	99.58	99.58	99.58	0.9958
	Without Oversampling	98.00	97.59	98.00	0.9770
RF	SMOTE	99.52	99.53	99.52	0.9952
	K-Means SMOTE	99.64	99.64	99.64	0.9964
	Borderline SMOTE	99.58	99.58	99.58	0.9958
	ADASYN	99.54	99.54	99.54	0.9953
	Without Oversampling	98.09	97.67	98.09	0.9763
MLP	SMOTE	89.89	90.07	89.89	0.8985
	K-Means SMOTE	59.84	73.31	59.84	0.5754
	Borderline SMOTE	95.44	95.53	95.44	0.9545
	ADASYN	88.19	88.44	88.19	0.8818
	Without Oversampling	97.61	96.00	97.61	0.9670
LSTM	SMOTE	69.02	69.09	69.01	0.6829



	K-Means SMOTE	78.56	78.98	78.55	0.7864
	Borderline SMOTE	86.23	86.52	86.22	0.8609
	ADASYN	76.78	77.06	76.77	0.7664
	Without Oversampling	97.79	95.63	97.78	0.9669
	SMOTE	99.58	99.58	99.58	0.9958
Dynamic Ensemble	K-Means SMOTE	99.68	99.68	99.68	0.9968
	Borderline SMOTE	99.55	99.55	99.55	0.9955
	ADASYN	99.58	99.58	99.58	0.9958
	Without Oversampling	98.20	97.83	98.20	0.9783

439 7. Discussion and Conclusions

440 In summary, the threat posed by landslides requires the development of effective prediction frameworks,
 441 although modelling the chaotic nature of natural data remains challenging. The analysed dataset exhibited a
 442 significant class imbalance, with the majority class dominating the samples. This distribution imbalance
 443 necessitated careful consideration and appropriate techniques to address the issue.

444 Various oversampling techniques, including SMOTE and its extensions (K-Means SMOTE, Borderline
 445 SMOTE, and SVM-SMOTE), were employed to tackle the class imbalance. ADASYN, which focuses on the
 446 minority class boundary, effectively generated synthetic data points, and improved the class distribution balance.

447 Multiple classification models, such as ADABOOST, XGBOOST, Light GBM, CatBoost, RF, MLP, LSTM, and
 448 a dynamic ensemble, were evaluated for predicting soil movement. The hyperparameters of each model were
 449 optimized using a grid search approach. The dynamic ensemble with K-Mean SMOTE and RF with K-Mean
 450 SMOTE emerged as the top-performing models, with the dynamic ensemble achieving slightly higher accuracy.

451 Combining K-Means SMOTE oversampling with the dynamic ensemble model yielded exceptional results,
 452 with high accuracy, precision, recall, and F1-score predicting soil movement. These outcomes demonstrate the
 453 effectiveness of oversampling techniques and the dynamic ensemble model in addressing class imbalance and
 454 improving landslide prediction accuracy.

455 This study emphasizes the importance of pre-processing, class labelling, addressing the class imbalance, and
 456 selecting suitable classification models for accurate soil movement prediction. The findings contribute to a better
 457 understanding of landslide risks and support the development of effective preventive measures.

458 However, there are several limitations to consider. The generalizability of the findings to other regions or
 459 geological conditions may be limited due to the specific dataset used. The synthetic data points generated
 460 through oversampling may only partially capture the complexity of real-world landslide occurrences. The choice
 461 of classification models and hyperparameter settings could introduce bias, and alternative configurations may
 462 yield different results. The study relied on historical data, potentially limiting its ability to account for future
 463 changes. Factors such as rainfall intensity, seismic activity, and human influences were not fully accounted for,
 464 suggesting the need for further research to enhance landslide prediction accuracy.

465 In future work, we plan to evaluate the performance of encoder-decoder models or transformer models on
 466 the class-imbalanced movement dataset. These models have demonstrated success in sequence-to-sequence
 467 tasks and could potentially improve classification accuracy and address class imbalance challenges. This
 468 experimentation will provide valuable insights into their suitability for analyzing and modeling imbalanced
 469 movement data.

470 Acknowledgements

471 We would like to acknowledge and express our sincere gratitude to the DST, India, and the DDMA Kangra
 472 (IITM/DDMA-Kan/KVU/357), Kinnaur (IITM/DDMA-Kinn/VD/345), and Mandi (IITM/DDMA-M/VD/325
 473 and IITM/DDMA-M/VD/358) for their invaluable financial support towards this research project. We are also
 474 immensely grateful to the IIT Mandi for generously facilitating us with the necessary infrastructure, including



475 research facilities and computational resources, that have been instrumental in the successful execution of this
476 study.

477 **References**

- 478 Breiman, L.: Random forests. *Machine learning*, 45, 5-32, 2001.
- 479 Chawla, N. V., Bowyer, K. W., Hall, L. O., & Kegelmeyer, W. P.: SMOTE: synthetic minority over-sampling
480 technique. *Journal of artificial intelligence research*, 16, 321-357, 2002.
- 481 Chen, T., & Guestrin, C.: Xgboost: A scalable tree boosting system. In Proceedings of the 22nd acm sigkdd international
482 conference on knowledge discovery and data mining, pp. 785-794, 2016.
- 483 Crosta, G.: Regionalization of rainfall thresholds: an aid to landslide hazard evaluation. *Environmental Geology*, 35(2), 131-
484 145, 1998.
- 485 Douzas, G., Bacao, F., & Last, F.: Improving imbalanced learning through a heuristic oversampling method based on k-
486 means and SMOTE. *Information Sciences*, 465, 1-20.
- 487 Han, H., Wang, W. Y., & Mao, B. H.: Borderline-SMOTE: a new over-sampling method in imbalanced data sets learning.
488 In Advances in Intelligent Computing: International Conference on Intelligent Computing, ICIC 2005, Hefei, China,
489 August 23-26, 2005, Proceedings, Part I 1, pp. 878-887, 2005.
- 490 He, H., Bai, Y., Garcia, E. A., & Li, S.: ADASYN: Adaptive synthetic sampling approach for imbalanced learning. In 2008
491 *IEEE international joint conference on neural networks (IEEE world congress on computational intelligence)*, pp.
492 1322-1328, 2008.
- 493 Hochreiter, S., & Schmidhuber, J.: Long short-term memory. *Neural computation*, 9(8), 1735-1780, 1997.
- 494 Ke, G., Meng, Q., Finley, T., Wang, T., Chen, W., Ma, W., ... & Liu, T. Y.: Lightgbm: A highly efficient gradient boosting
495 decision tree. *Advances in neural information processing systems*, 30, 2017.
- 496 Ko, A. H., Sabourin, R., & Britto Jr, A. S.: From dynamic classifier selection to dynamic ensemble selection. *Pattern
497 recognition*, 41(5), 1718-1731, 2008.
- 498 Kumar, P., Sihag, P., Sharma, A., Pathania, A., Singh, R., Chaturvedi, P., & Dutt, V.: Prediction of Real-World Slope
499 Movements via Recurrent and Non-recurrent Neural Network Algorithms: A Case Study of the Tangni
500 Landslide. *Indian Geotechnical Journal*, 51(4), 788-810 (2021a).
- 501 Kumar, P., Sihag, P., Chaturvedi, P., Uday, K. V., & Dutt, V.: BS-LSTM: an ensemble recurrent approach to forecasting soil
502 movements in the real world. *Frontiers in Earth Science*, 9, 696-792 (2021b).
- 503 Kumar, P., Sihag, P., Pathania, A., Agarwal, S., Mali, N. C. P., Singh, R., ... & Dutt, V.: Landslide debris-flow prediction
504 using ensemble and non-ensemble machine-learning methods. In *International Conference on Time Series and
505 Forecasting* (Vol. 1), 2019.
- 506 Kumar, P., Priyanka, Pathania, A., Agarwal, S., Mali, N., Singh, R., ... & Dutt, V.: Predictions of weekly slope movements
507 using moving-average and neural network methods: a case study in Chamoli, India. In *Soft Computing for Problem
508 Solving 2019: Proceedings of SocProS 2019, Volume 2*, pp. 67-81, 2020.
- 509 Parkash, S.: Historical records of socio-economically significant landslides in India. *Journal of South Asia Disaster Studies*,
510 4(2), 177-204, 2011.
- 511 Pathania, A., Kumar, P., Priyanka, P., Maurya, A., Uday, K. V., & Dutt, V.: Development of an Ensemble Gradient Boosting
512 Algorithm for Generating Alerts About Impending Soil Movements. In *Machine Learning, Deep Learning and
513 Computational Intelligence for Wireless Communication: Proceedings of MDCWC 2020*, pp. 365-379, 2021.
- 514 Pathania, A., Kumar, P., Sihag, P., Chaturvedi, P., Singh, R., Uday, K. V., & Dutt, V.: A low-cost, sub-surface IoT framework
515 for landslide monitoring, warning, and prediction. In *Proceedings of 2020 International conference on advances in
516 computing, communication, embedded and secure systems*, 2020.
- 517 Prokhorenkova, L., Gusev, G., Vorobev, A., Drogush, A. V., & Gulin, A.: CatBoost: unbiased boosting with categorical
518 features. *Advances in neural information processing systems*, 31, 2018.
- 519 Ray, R. L., Lazzari, M., & Olutimehin, T.: Remote sensing approaches and related techniques to map and study
520 landslides. *Landslides Investig. Monit.*, 2020.



- 521 Rosenblatt, F.: Principles of neurodynamics. perceptrons and the theory of brain mechanisms. *Cornell Aeronautical Lab Inc*
522 *Buffalo NY*, 1961.
- 523 Sahin, E. K.: Comparative analysis of gradient boosting algorithms for landslide susceptibility mapping. *Geocarto*
524 *International*, 37(9), 2441-2465, 2022.
- 525 Semwal, T., Priyanka, P., Kumar, P., Dutt, V., & Uday, K. V.: Predictions of Root Tensile Strength for Different Vegetation
526 Species Using Individual and Ensemble Machine Learning Models. In *Trends on Construction in the Digital Era:*
527 *Proceedings of ISIC 2022*, pp. 87-100, 2022.
- 528 Tang, Y., Zhang, Y. Q., Chawla, N. V., & Krasser, S.: SVMs modeling for highly imbalanced classification. *IEEE*
529 *Transactions on Systems, Man, and Cybernetics, Part B (Cybernetics)*, 39(1), 281-288, 2008.
- 530 Wu, Y., Ke, Y., Chen, Z., Liang, S., Zhao, H., & Hong, H.: Application of alternating decision tree with AdaBoost and
531 bagging ensembles for landslide susceptibility mapping. *Catena*, 187, 104396, 2020.
- 532 Zhang, S., Wang, Y., & Wu, G.: Earthquake-Induced Landslide Susceptibility Assessment Using a Novel Model Based on
533 Gradient Boosting Machine Learning and Class Balancing Methods. *Remote Sensing*, 14(23), 5945, 2022.